Calhoun
Institutional Archive of the Naval Postgraduate School

Calhoun: The NPS Institutional Archive

DSpace Repository

Faculty and Researchers | Faculty and Researchers' Publications

1989

Localization of multiple broadband targets via frequency domain adaptive beamforming for planar arrays

Ziomek, Lawrence J.; Behrle, Charles D.

Acoustical Society of America

The Journal of the Acoustical Society of America 85, 1236 (1989); https://doi.org/10.1121/1.397454
http://hdl.handle.net/10945/59972

This publication is a work of the U.S. Government as defined in Title 17, United States Code, Section 101. Copyright protection is not available for this work in the United States.

Downloaded from NPS Archive: Calhoun

http://www.nps.edu/library

Calhoun is the Naval Postgraduate School's public access digital repository for research materials and institutional publications created by the NPS community. Calhoun is named for Professor of Mathematics Guy K. Calhoun, NPS's first appointed -- and published -- scholarly author.

Dudley Knox Library / Naval Postgraduate School
411 Dyer Road / 1 University Circle
Monterey, California USA 93943

Localization of multiple broadband targets via frequency domain adaptive beamforming for planar arrays[a)]

Lawrence J. Ziomek and Charles D. Behrle
Department of Electrical and Computer Engineering, Naval Postgraduate School, Monterey, California 93943

(Received 4 April 1988; accepted for publication 21 October 1988)

Computer simulation studies of a frequency domain adaptive beamforming algorithm for *planar arrays* are presented. The algorithm, which can localize *multiple broadband targets*, is a modified complex least-mean-square (LMS) adaptive algorithm, and can process an arbitrary number of harmonics. The algorithm provides estimates of *both* the depression and bearing angles of incident plane-wave fields. Computer simulation results are presented comparing the *average* depression and bearing angle estimation errors as a function of the input signal-to-noise ratio (SNR) at a single element in the array, sampling rate, and harmonic number. The "full angular coverage" capability of the algorithm was also tested.

PACS numbers: 43.60.Gk, 43.30.Wi

INTRODUCTION

The purpose of this article is to present the results of computer simulation studies of a frequency domain adaptive beamforming algorithm for *planar arrays* that can be used to localize *multiple broadband targets*. The algorithm[1,2] is a modified complex least-mean-square (LMS) adaptive algorithm[3] that processes the output complex frequency domain data from all $M \times N$ elements in a planar array in order to provide estimates of *both* the depression and bearing (azimuthal) angles θ_0 and ψ_0, respectively, of incident plane-wave fields (see Fig. 1). As a result, an estimate of the direction to a target (or targets), as measured from the center of the planar array, can be obtained. In contrast, several recent papers[4–6] have discussed the application of the complex LMS adaptive algorithm[3] to bearing estimation problems using a linear array of sensors. For example, when a horizontal linear array lying along the X axis is used, only the direction cosine in the X direction, u_0, can be estimated [see Eqs. (2)–(11) and Fig. 1]. The problem is that u_0 depends on *both* the depression angle θ_0 and the bearing angle ψ_0; that is, there is only one equation but two unknowns. Only if it is assumed that θ_0 has some value, for example, $\theta_0 = \pi/2$ (see Fig. 1), can a unique estimate of ψ_0 be obtained. In addition, there is the problem of quadrant ambiguity when using a horizontal linear array to estimate bearing angles.

In this article, each target was modeled as a *broadband* sound source. As a result, the complex frequency spectrum of the output signal from each element in the array contains many frequency components. Since *each* frequency component is processed by the frequency domain adaptive beamforming algorithm, depression and bearing angle estimates are associated with each frequency component. Therefore, if each target contains at least one unique spectral line, then the adaptive algorithm can localize all of the targets. This last requirement is reasonable since several supposedly identical sound sources are *not* exactly identical in practice. Furthermore, the fast Fourier transform (FFT) bin spacing can be made as small as desired to ensure at least one unique spectral line per target. The FFT bin spacing is also important when processing data from broadband targets since significant spectral lines may be missed if the bin spacing (i.e., the fundamental frequency) is too large.

The computer simulation studies performed were designed to test the algorithm's multiple target capability, its full angular coverage capability, and its angular resolution as a function of the input SNR at a single element in the array, sampling rate, harmonic number, and the number of iterations of the algorithm. Baseline results, that is, depression and bearing angle estimation errors as a function of the sampling rate, harmonic number, and the number of iterations of the algorithm for the "no noise" cases, were compiled first.

Full angular coverage is the ability to localize a target whether it is at broadside or at end-fire relative to the array. This is easier in the broadside case since the beamwidth of the farfield beam pattern of the planar array is smallest at broadside and harder in the end-fire case since the beamwidth is largest at end-fire. The multiple broadband target and full angular coverage capabilities of the adaptive beamforming algorithm were tested simultaneously since multi-

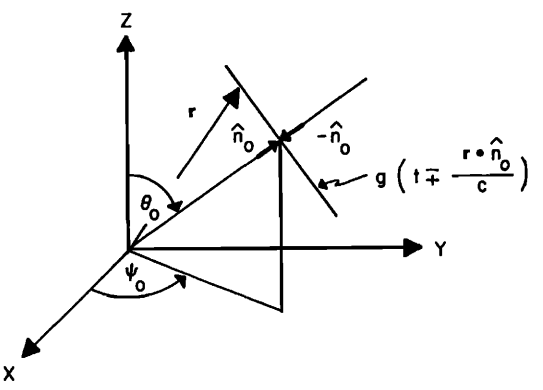

FIG. 1. General plane-wave field $g(t \mp \mathbf{r}\cdot\hat{n}_0/c)$ propagating in the $\pm\hat{n}_0$ direction.

[a)] Portions of this article were presented at the 21st Annual Asilomar Conference on Signals, Systems, and Computers, 2–4 November, 1987, Pacific Grove, CA.

ple targets, each with several different frequency components, were placed at different spatial locations relative to the array.

Once the baseline results were obtained, identical test cases were run using additive, zero mean, white, Gaussian noise to corrupt the output signals from each element in the planar array. *Average* depression and bearing angle estimation errors (in degrees) were then plotted as a function of the input SNR at a single element in the array, the sampling rate, and the harmonic number.

I. ANALYSIS

Consider a planar array of $M \times N$ (odd), equally spaced, point source elements lying in the XY plane, where M and N are the total odd number of elements in the X and Y directions, respectively. Let the random output electrical signal received at time instant l and element (m,n) in the array be given by

$$\begin{aligned} r(l,m,n) &= y(l,m,n) + z(l,m,n), \\ & l = -L',...,0,...,L', \\ & m = -M',...,0,...,M', \\ & n = -N',...,0,...,N', \end{aligned} \tag{1}$$

where $y(l,m,n)$ and $z(l,m,n)$ are the deterministic signal and random receiver noise, respectively,

$$L' = (L-1)/2, \tag{2}$$

$$M' = (M-1)/2, \tag{3}$$

$$N' = (N-1)/2, \tag{4}$$

and

$$L \geqslant 2K+1 \tag{5}$$

is the total number of time samples that must be taken per element in order to avoid aliasing when the signal $y(l,m,n)$ is composed of K harmonics.[7] If we designate the length of the data record (i.e., the fundamental period) recorded at each element in the array as T_0 s, then the fundamental frequency (i.e., the FFT bin spacing) is $f_0 = 1/T_0$ Hz, the highest frequency component contained in $y(l,m,n)$ is Kf_0 Hz, and the output received signals $r(l,m,n)$ must be sampled at a rate of

$$f_s = L/T_0 \text{ samples/s}, \tag{6}$$

where L is given by Eq. (5).[7] Taking the discrete Fourier transform (DFT) of Eq. (1), with respect to the time index l, yields the complex frequency domain samples

$$\begin{aligned} R(q,m,n) &= Y(q,m,n) + Z(q,m,n), \\ & q = -L',...,0,...,L', \\ & m = -M',...,0,...,M', \\ & n = -N',...,0,...,N', \end{aligned} \tag{7}$$

where the index q represents the harmonic number. If the acoustic field incident upon the planar array is a *single* general plane-wave field $g[t \mp (\mathbf{r}\cdot\hat{n}_0)/c]$ propagating in the $\pm\hat{n}_0$ direction (see Fig. 1), where $\hat{n}_0$ is a unit vector and $g(t)$ is an arbitrary function of time, then it can be shown that the output electrical signal at time instant l and element (m,n) in the array is given by[8]

$$y(l,m,n) = g[lT_s \mp (u_0 m d_X + v_0 n d_Y)/c], \tag{8}$$

with corresponding frequency spectrum given by[7]

$$\begin{aligned} Y(q,m,n) = Lc_q & \exp(\mp j2\pi q f_0 u_0 m d_X/c) \\ & \times \exp(\mp j2\pi q f_0 v_0 n d_Y/c), \end{aligned} \tag{9}$$

where

$$c_q = Y(q,0,0)/L, \quad q = -L',...,0,...,L' \tag{10}$$

are the complex Fourier series coefficients that can be used to represent $g(t)$ by a finite Fourier series with K harmonics during the time interval $|t| \leqslant T_0/2$, $f_0 = 1/T_0$,

$$u_0 = \sin\theta_0 \cos\psi_0 \tag{11}$$

and

$$v_0 = \sin\theta_0 \sin\psi_0 \tag{12}$$

are the dimensionless direction cosines with respect to the X and Y axes, respectively, θ_0 and ψ_0 are the depression and bearing angles, respectively, d_X and d_Y are the interelement spacings in meters in the X and Y directions, respectively, and c is the speed of sound in meters per second.

Equation (9) is the basis for the frequency domain adaptive beamforming algorithm to be presented in this article. Since Eq. (9) was obtained via a time domain DFT of Eq. (8), the algorithm represents a nonparametric approach to multiple target localization problems.[9] However, unlike the approach of using a horizontal linear array to estimate the angles of arrival ψ_0 of multiple incident plane-wave fields at the same frequency by locating their corresponding peaks in the angular spectrum (wavenumber spectrum) (e.g., see Refs. 10 and 11), the algorithm presented in this article uses a planar array to estimate *both* angles θ_0 and ψ_0 for *each* harmonic q present in the multiple incident plane-wave fields via frequency domain adaptive beamforming. Therefore, in this article, we shall use the following generalized version of Eq. (8):

$$y(l,m,n) = \sum_k g_k\left(lT_s \mp \frac{u_{0k} m d_X + v_{0k} n d_Y}{c}\right), \tag{13}$$

which represents the output electrical signal at time instant l and element (m,n) in the planar array due to *several* incident plane-wave fields, where $g_k(t)$, u_{0k}, and v_{0k} are the arbitrary function of time and direction cosines associated with the k th sound source (target), respectively. It shall be shown that the frequency domain adaptive beamforming algorithm will be able to localize all targets *if each* $g_k(t)$ *is unique*, that is, if each sound source contains at least one unique spectral line.

The frequency domain adaptive beamforming algorithm to be discussed is based on processing the output complex frequency domain data $R(q,m,n)$ from *all* $M \times N$ elements in the planar array. We begin by defining the complex estimation error as

$$e(q) \triangleq s(q) - \hat{s}(q), \tag{14}$$

where

$$\begin{aligned} s(q) \triangleq \frac{1}{LMN} & \sum_{m=-M'}^{M'} \sum_{n=-N'}^{N'} |R(q,m,n)| \\ & \times \exp[+j\angle R(q,0,0)] \end{aligned} \tag{15}$$

is defined as the reference signal and

$$\hat{s}(q) \triangleq \frac{1}{LMN} \sum_{m=-M'}^{M'} \sum_{n=-N'}^{N'} c(q,m)d(q,n)R(q,m,n)$$
$$= \mathbf{c}^T(q)\mathbf{R}(q)\mathbf{d}(q)/(LMN) \quad (16)$$

is defined as the estimate of $s(q)$. In addition, $c(q,m)$ and $d(q,n)$ are the *unit magnitude* complex weights in the X and Y directions, respectively, $\mathbf{c}(q)$ and $\mathbf{d}(q)$ are the $M \times 1$ and $N \times 1$ complex weight vectors in the X and Y directions, respectively, given by

$$\mathbf{c}(q) = [c(q,-M'),...,c(q,0),...,c(q,M')]^T \quad (17)$$

and

$$\mathbf{d}(q) = [d(q,-N'),...,d(q,0),...,d(q,N')]^T, \quad (18)$$

respectively, and

$$\mathbf{R}(q) = \begin{bmatrix} R(q,-M',-N') & \cdots & R(q,-M',0) & \cdots & R(q,-M',N') \\ \vdots & & \vdots & & \vdots \\ R(q,0,-N') & \cdots & R(q,0,0) & \cdots & R(q,0,N') \\ \vdots & & \vdots & & \vdots \\ R(q,M',-N') & \cdots & R(q,M',0) & \cdots & R(q,M',N') \end{bmatrix} \quad (19)$$

is the $M \times N$ complex data matrix. Next, define the $(M+N) \times 1$ complex weight vector $\mathbf{w}(q)$ as follows:

$$\mathbf{w}(q) \triangleq \begin{bmatrix} \mathbf{c}(q) \\ \mathbf{d}(q) \end{bmatrix}. \quad (20)$$

Therefore,

$$\mathbf{c}(q) = \mathbf{A}\mathbf{w}(q), \quad (21)$$

where

$$\mathbf{A} = \begin{bmatrix} \mathbf{I}_{M \times M} & \mathbf{0}_{M \times N} \end{bmatrix} \quad (22)$$

is an $M \times (M+N)$ matrix, $\mathbf{I}$ is an $M \times M$ identity matrix, $\mathbf{0}$ is an $M \times N$ null matrix as indicated, and

$$\mathbf{d}(q) = \mathbf{B}\mathbf{w}(q), \quad (23)$$

where

$$\mathbf{B} = \begin{bmatrix} \mathbf{0}_{N \times M} & \mathbf{I}_{N \times N} \end{bmatrix} \quad (24)$$

is an $N \times (M+N)$ matrix, $\mathbf{0}$ is an $N \times M$ null matrix, and $\mathbf{I}$ is an $N \times N$ identity matrix as indicated. Substituting Eqs. (21) and (23) into Eq. (16) yields

$$\hat{s}(q) = \mathbf{w}^T(q)\mathbf{Z}(q)\mathbf{w}(q)/(LMN), \quad (25)$$

where

$$\mathbf{Z}(q) = \mathbf{A}^T\mathbf{R}(q)\mathbf{B} \quad (26)$$

is a $(M+N) \times (M+N)$ complex matrix. The complex weight vector that minimizes the mean-square error $E\{|e(q)|^2\}$ is given by[2]

$$\mathbf{w}_{i+1}(q) = \mathbf{w}_i(q) + 2\mu_i e_i(q)[\mathbf{Z}(q) + \mathbf{Z}^T(q)]^* \mathbf{w}_i^*(q), \quad i = 0,1,2,..., \quad (27)$$

where

$$e_i(q) = s(q) - \hat{s}_i(q) \quad (28)$$

is the estimation error after the ith iteration,

$$\hat{s}_i(q) = \mathbf{w}_i^T(q)\mathbf{Z}(q)\mathbf{w}_i(q)/(LMN) \quad (29)$$

is the estimate of $s(q)$ after the ith iteration, and, in this article, the step-size parameter μ_i is given by

$$\mu_i = \mu_0 = (\sigma_y^2 + \sigma_n^2)^{-1}, \quad i = 0,1,2,..., \quad (30)$$

where μ_0 is *constant* and σ_y^2 and σ_n^2 are the signal and noise power, respectively, at the center element in the array. Note that choosing the step-size parameter μ_0 to be a *constant* allows the LMS algorithm to operate in a nonstationary time-domain environment.[12] After each iteration, each component of the complex weight vector $\mathbf{w}_{i+1}(q)$ is normalized by its respective magnitude in order to maintain unit magnitude.

Once the complex weight vector $\mathbf{w}_{i+1}(q)$ converges to a steady-state value $\mathbf{w}_{SS}(q)$, the steady-state complex weight vectors $\mathbf{c}_{SS}(q)$ and $\mathbf{d}_{SS}(q)$ can be obtained from Eqs. (21) and (23), respectively. The estimates of $\theta_0(q)$ and $\psi_0(q)$ at each harmonic q are given by[13]

$$\hat{\theta}_0(q) = \sin^{-1}(\{[\hat{u}_0^{LS}(q)]^2 + [\hat{v}_0^{LS}(q)]^2\}^{1/2}), \quad q \neq 0 \quad (31)$$

and

$$\hat{\psi}_0(q) = \tan^{-1}[\hat{v}_0^{LS}(q)/\hat{u}_0^{LS}(q)], \quad q \neq 0, \quad (32)$$

where $\hat{u}_0^{LS}(q)$ and $\hat{v}_0^{LS}(q)$ represent estimates of the direction cosines obtained by using a *least-squares fit* to the "unwrapped" steady-state phase weights $\theta_{SS}^U(q,m)$ and $\phi_{SS}^U(q,n)$, respectively. Note that in the *absence of noise*,

$$\theta_{SS}^U(q,m) = \pm 2\pi q f_0 u_0(q) m d_X/c, \quad q = -L',...,0,...,L', \quad m = -M',...,0,...,M', \quad (33)$$

and

$$\phi_{SS}^U(q,n) = \pm 2\pi q f_0 v_0(q) n d_Y/c, \quad q = -L',...,0,...,L', \quad n = -N',...,0,...,N'. \quad (34)$$

The steady-state phase weights need to be unwrapped, that is, allowed to take on values outside the closed interval $[-\pi,\pi]$ in order to ensure full angular coverage (i.e., $0 \leqslant \theta_0(q) \leqslant \pi/2$ and $0 \leqslant \psi_0(q) \leqslant 2\pi$) and correct depression and bearing angle estimates $\hat{\theta}_0(q)$ and $\hat{\psi}_0(q)$, respectively. Finally, substituting Eqs. (15) and (16) into Eq. (14) yields the following expression for the steady-state estimation error:

$$e_{SS}(q) = \frac{1}{LMN} \sum_{m=-M'}^{M'} \sum_{n=-N'}^{N'} |R(q,m,n)| \times \{\exp[+j \angle R(q,0,0)]$$

$$- \exp\{ +j[\theta^W_{SS}(q,m) + \phi^W_{SS}(q,n) + \angle R(q,m,n)]\}, \quad (35)$$

where

$$R(q,m,n) = |R(q,m,n)|\exp[+j\angle R(q,m,n)], \quad (36)$$

$$c_{SS}(q,m) = a_{SS}(q,m)\exp[+j\theta^W_{SS}(q,m)] = \exp[+j\theta^W_{SS}(q,m)], \quad (37)$$

and

$$d_{SS}(q,n) = b_{SS}(q,n)\exp[+j\phi^W_{SS}(q,n)] = \exp[+j\phi^W_{SS}(q,n)], \quad (38)$$

where $a_{SS}(q,m) = 1$ and $b_{SS}(q,n) = 1$ are real, unit magnitude, amplitude weights, and $\theta^W_{SS}(q,m)$ and $\phi^W_{SS}(q,n)$ are real, "wrapped" phase weights.

Let us conclude this part of the article by discussing how we unwrapped the steady-state phase weights in order to obtain least-squares estimates of the direction cosines at each harmonic. The first step was to force the wrapped steady-state phase weights (phase weights whose values are confined to the closed interval $[-\pi,\pi]$) $\theta^W_{SS}(q,m)$ and $\phi^W_{SS}(q,n)$ to be equal to zero at the center element of the planar array, that is, at $m = 0$ and $n = 0$, respectively. This was accomplished by multiplying each component of the steady-state complex weight vectors $\mathbf{c}_{SS}(q)$ and $\mathbf{d}_{SS}(q)$ [see Eqs. (17) and (18), respectively] by $\exp[-j\theta^W_{SS}(q,0)]$ and $\exp[-j\phi^W_{SS}(q,0)]$, respectively.

The second step was to obtain *rough estimates* of both direction cosines at each harmonic. Consider direction cosine $u_0(q)$. The wrapped steady-state phase weight $\theta^W_{SS}(q,m)$ can be expressed as

$$\theta^W_{SS}(q,m) \approx \pm [2\pi q f_0 u_0(q) m d_X/c] + 2i\pi, \quad i = 0, \pm 1, \pm 2,\ldots, \quad q = -L',\ldots,0,\ldots,L', \quad m = -M',\ldots,0,\ldots,M', \quad (39)$$

where the integer i is chosen so that the value of $\theta^W_{SS}(q,m)$ is confined to the closed interval $[-\pi,\pi]$. Since in this article

$$d_X = d_Y = \lambda_{min}/2, \quad (40)$$

where

$$\lambda_{min} = c/f_{max}, \quad (41)$$

and, since

$$f_{max} = L' f_0, \quad (42)$$

substituting Eqs. (41) and (42) into Eq. (40) yields

$$d_X = d_Y = c/(2L' f_0), \quad (43)$$

where L' is given by Eq. (2) and $f_0 = 1/T_0$. Substituting Eq. (43) into Eq. (39) yields

$$\theta^W_{SS}(q,m) \approx \pm (q/L')mu_0(q)\pi + 2i\pi, \quad i = 0, \pm 1, \pm 2,\ldots, \quad q = -L',\ldots,0,\ldots,L', \quad m = -M',\ldots,0,\ldots,M', \quad (44)$$

and, upon setting $i = 0$ in Eq. (44), we can write that

$$\hat{u}_0(q,m) = \pm (L'/qm\pi)\theta^W_{SS}(q,m), \quad q \neq 0, \quad m = \pm 1, \quad (45)$$

which is the rough estimate of u_0 at harmonic q and element m. The rough estimate of $u_0(q)$ used in this article was obtained by averaging the results obtained by evaluating Eq. (45) at elements $m = \pm 1$; that is,

$$\hat{u}_0(q) = 0.5[\hat{u}_0(q,1) + \hat{u}_0(q,-1)], \quad q \neq 0. \quad (46)$$

The reason for limiting the evaluation of Eq. (45) to $m = \pm 1$ is explained next by means of an example. The worst case from an angular coverage point of view corresponds to the highest harmonic $q = L'$ existing at end-fire; that is, $u_0(L') = \pm 1$ (similarly, for $q = -L'$, $u_0(-L') = \pm 1$). Therefore, if we choose the plus sign in Eq. (44) and assume *no noise* for example purposes, and, if we evaluate Eq. (44) at $q = L'$ with $u_0(L') = +1$, then Eq. (44) reduces to

$$\theta^W_{SS}(L',m) = m\pi + 2i\pi, \quad i = 0, \pm 1, \pm 2,\ldots, \quad m = -M',\ldots,0,\ldots,M'. \quad (47)$$

Evaluating Eq. (47) at $m = \pm 1$ yields

$$\theta^W_{SS}(L', \pm 1) = \pm \pi + 2i\pi, \quad i = 0, \pm 1, \pm 2,\ldots, \quad (48)$$

and, in order to confine the value of Eq. (48) to the closed interval $[-\pi,\pi]$, we choose $i = 0$ so that

$$\theta^W_{SS}(L', \pm 1) = \pm \pi. \quad (49)$$

Accordingly, if we choose the plus sign in Eq. (45), and, if we evaluate Eq. (45) at $q = L'$ and $m = \pm 1$, then

$$\hat{u}_0(L', \pm 1) = \theta^W_{SS}(L', \pm 1)/(\pm \pi), \quad (50)$$

and, upon substituting Eq. (49) into Eq. (50), we obtain $\hat{u}_0(L', \pm 1) = 1$. If we then substitute this result into Eq. (46), we finally obtain $\hat{u}_0(L') = 1$, which is the correct answer (in the absence of noise), since it was assumed that $u_0(L') = 1$ in this example. Evaluating Eq. (47) at any elements other than $m = \pm 1$ in this example would yield $i \neq 0$ and, as a result, Eq. (46) would ultimately give an *incorrect* rough estimate of $u_0(L')$.

The next step was to generate rough estimates of the unwrapped steady-state phase weights, $\hat{\theta}^U_{SS}(q,m)$, by replacing $u_0(q)$ in Eq. (44) with $\hat{u}_0(q)$ from Eq. (46), that is,

$$\hat{\theta}^U_{SS}(q,m) = \pm (q/L')m\hat{u}_0(q)\pi, \quad q = -L',\ldots,0,\ldots,L', \quad m = -M',\ldots,0,\ldots,L'. \quad (51)$$

Therefore, if

$$i\pi < |\hat{\theta}^U_{SS}(q,m)| \leqslant (i+2)\pi, \quad i = 1,3,5,\ldots, \quad q = -L',\ldots,0,\ldots,L', \quad m = -M',\ldots,0,\ldots,M', \quad (52)$$

then we define the unwrapped steady-state phase weights as follows:

$$\theta^U_{SS}(q,m) \triangleq \theta^W_{SS}(q,m) + \mathrm{sgn}[\hat{\theta}^U_{SS}(q,m)](i+1)\pi,$$

$$i = 1,3,5,\ldots,$$
$$q = -L',\ldots,0,\ldots,L',$$
$$m = -M',\ldots,0,\ldots,M', \tag{53}$$

where sgn[ ] is the signum or sign function. Note that the right-hand side of Eq. (53) is simply the noise-corrupted version of the right-hand side of Eq. (33).

The method of least squares was then used to fit a straight line to the unwrapped steady-state phase weights $\theta_{SS}^{U}(q,m)$, computed using Eq. (53), as a function of element number m for each harmonic q. The least-squares slope at harmonic q is given by

$$\hat{s}_{LS}(q) = \sum_{m=-M'}^{M'} m\theta_{SS}^{U}(q,m) \Big/ \sum_{m=-M'}^{M'} m^2. \tag{54}$$

Substituting Eq. (43) into Eq. (33) yields

$$\theta_{SS}^{U}(q,m) = \pm (q/L')\pi u_0(q)m,$$
$$q = -L',\ldots,0,\ldots,L',$$
$$m = -M',\ldots,0,\ldots,M', \tag{55}$$

in the *absence of noise*. Therefore, since in the presence of noise

$$\theta_{SS}^{U}(q,m) \approx \hat{s}_{LS}(q)m + \hat{b}_{LS}(q),$$
$$q = -L',\ldots,0,\ldots,L',$$
$$m = -M',\ldots,0,\ldots,M', \tag{56}$$

where

$$\hat{b}_{LS}(q) = \frac{1}{M}\sum_{m=-M'}^{M'} \theta_{SS}^{U}(q,m) \tag{57}$$

is the least-squares "y intercept" at harmonic q, comparing Eqs. (55) and (56) yields

$$\pm \hat{u}_0^{LS}(q) = [L'/(q\pi)]\hat{s}_{LS}(q), \quad q \neq 0, \tag{58}$$

which is the *least-squares estimate* of direction cosine $u_0(q)$ at harmonic q.

In a similar fashion, it can be shown that the *least-squares estimate* of direction cosine $v_0(q)$ at harmonic q is given by

$$\pm \hat{v}_0^{LS}(q) = [L'/(q\pi)]\hat{s}_{LS}(q), \quad q \neq 0, \tag{59}$$

where, now,

$$\hat{s}_{LS}(q) = \sum_{n=-N'}^{N'} n\phi_{SS}^{U}(q,n) \Big/ \sum_{n=-N'}^{N'} n^2, \tag{60}$$

and, if

$$i\pi < |\hat{\phi}_{SS}^{U}(q,n)| \leq (i+2)\pi,$$
$$i = 1,3,5,\ldots,$$
$$q = -L',\ldots,0,\ldots,L',$$
$$n = -N',\ldots,0,\ldots,N', \tag{61}$$

then, by definition

$$\phi_{SS}^{U}(q,n) \triangleq \phi_{SS}^{W}(q,n) + \text{sgn}[\hat{\phi}_{SS}^{U}(q,n)](i+1)\pi,$$
$$i = 1,3,5,\ldots,$$
$$q = -L',\ldots,0,\ldots,L',$$
$$n = -N',\ldots,0,\ldots,N', \tag{62}$$

where

$$\hat{\phi}_{SS}^{U}(q,n) = \pm (q/L')n\hat{v}_0(q)\pi,$$
$$q = -L',\ldots,0,\ldots,L',$$
$$n = -N',\ldots,0,\ldots,N', \tag{63}$$

$$\hat{v}_0(q) = 0.5[\hat{v}_0(q,1) + \hat{v}_0(q,-1)], \quad q \neq 0, \tag{64}$$

and

$$\hat{v}_0(q,n) = \pm (L'/qn\pi)\,\phi_{SS}^{W}(q,n),$$
$$q \neq 0, \quad n = \pm 1. \tag{65}$$

The least-squares estimates obtained from Eqs. (58) and (59) are then substituted into Eqs. (31) and (32) in order to obtain estimates of the depression and bearing angles at each harmonic.

II. SIMULATION RESULTS

The computer simulation results presented in this section are based on processing the output electrical signals from a 7×7 planar array of hydrophones. The acoustic field incident upon the array is, in general, equal to the sum of several general plane-wave fields, each traveling in different directions, and each composed of an arbitrary number of harmonics (spectral lines), due to the acoustic radiation from several broadband targets. Therefore, the output electrical signal at each element in the array is, in general, composed of an arbitrary number K of harmonics.

In all test cases, the fundamental frequency was chosen to be $f_0 = 1$ kHz, which implies that the fundamental period or, equivalently, the data record length at each element in the array was $T_0 = 1$ ms. The number of time samples taken per element in the array was [see Eq. (5)]

$$L = SK + 1, \tag{66}$$

where the *sampling parameter* S was set equal to 2, 4, and 6, which corresponds to sampling the output electrical signal from each element in the array at two, four, and six times the highest frequency component, respectively, where K is the total number of harmonics present. Note that $S = 2$ corresponds to the Nyquist rate. All harmonics (spectral lines) had identical amplitudes of unity.

In all of the baseline or "no noise" cases, except case 4, *the estimation errors were either zero or less than 0.1°*. For each no noise test case and, for a given value of S, depression and bearing angle estimation errors were obtained by running the computer simulation *once* and allowing the modified complex LMS algorithm 100 iterations.

Once the baseline results were obtained, identical test cases were run using additive, wide-sense stationary, zero mean, white, Gaussian noise samples to corrupt the time samples of the signal. For each test case and, for a given value of S and input SNR at a single element in the array, *average* depression and bearing angle estimation errors were obtained by running the computer simulation 100 times per SNR value and the modified complex LMS algorithm 100 iterations per run. In all cases, increasing the number of iterations of the modified complex LMS algorithm from 100 had no effect on the estimation errors.

Case 1 corresponds to only *one* broadband target being

present, located at *broadside* relative to the planar array, that is, located at $\theta_0 = 0°$. The general plane-wave field radiated by the target was composed of $K = 6$ harmonics. Therefore, with $K = 6$ and $S = 2$, 4, and 6, *only* $L = 13$, 25, and 37 time samples, respectively, were taken per element in the array [see Eq. (66)]. Figure 2(a) and (b) illustrates that for a given input SNR value and harmonic number q, the average depression angle estimation errors *decreased* as the sampling parameter value S *increased*. Similarly, for a given value of S, estimation errors *decreased* as harmonic number q *increased*. These results are not surprising since as the number of time samples increases, that is, as one processes more data, the tendency for the noise to average out to zero increases. Also, as harmonic number q (frequency) increases, the beamwidth of the farfield beam pattern decreases and, as a result, angular resolution increases. Since the adaptive beamforming algorithm described in this article forces all of the amplitude weights to be equal to unity, the 3-dB beamwidth of the untilted farfield beam pattern of the 7×7 planar

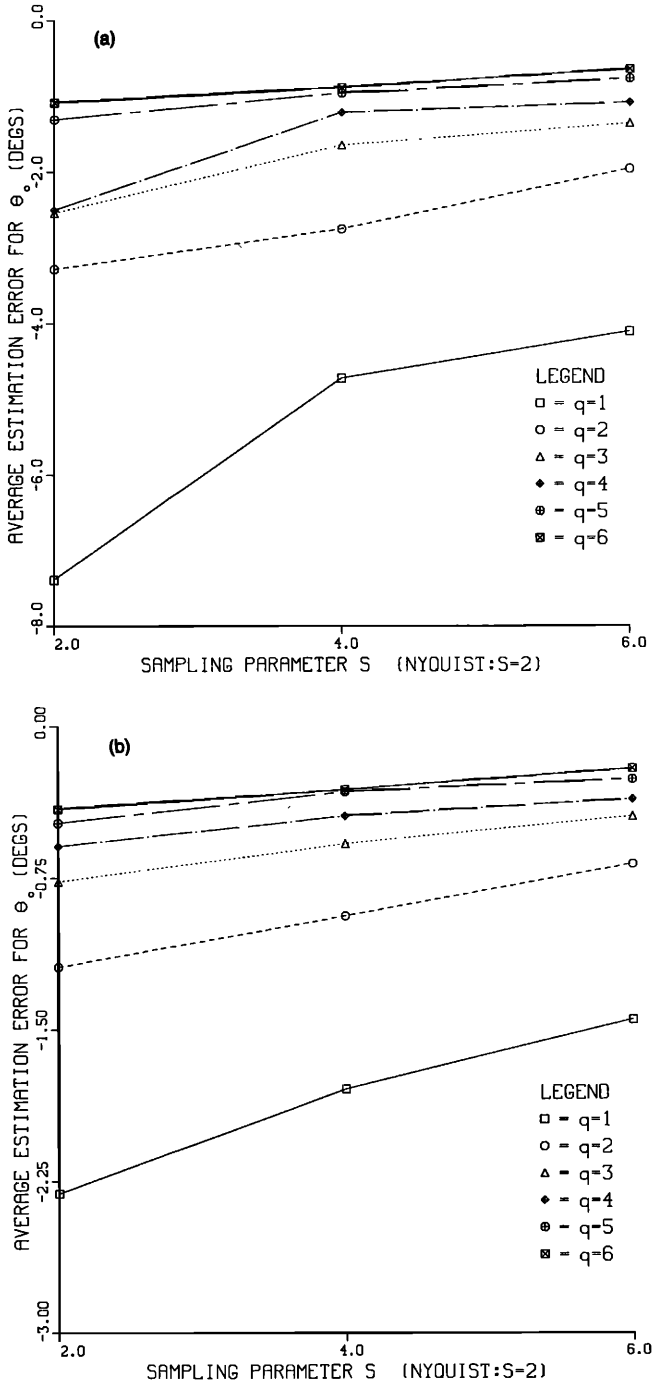

FIG. 2. Average estimation error versus sampling parameter S: (a) case 1: SNR = 0 dB, $I = 100$; (b) case 1: SNR = 9 dB, $I = 100$.

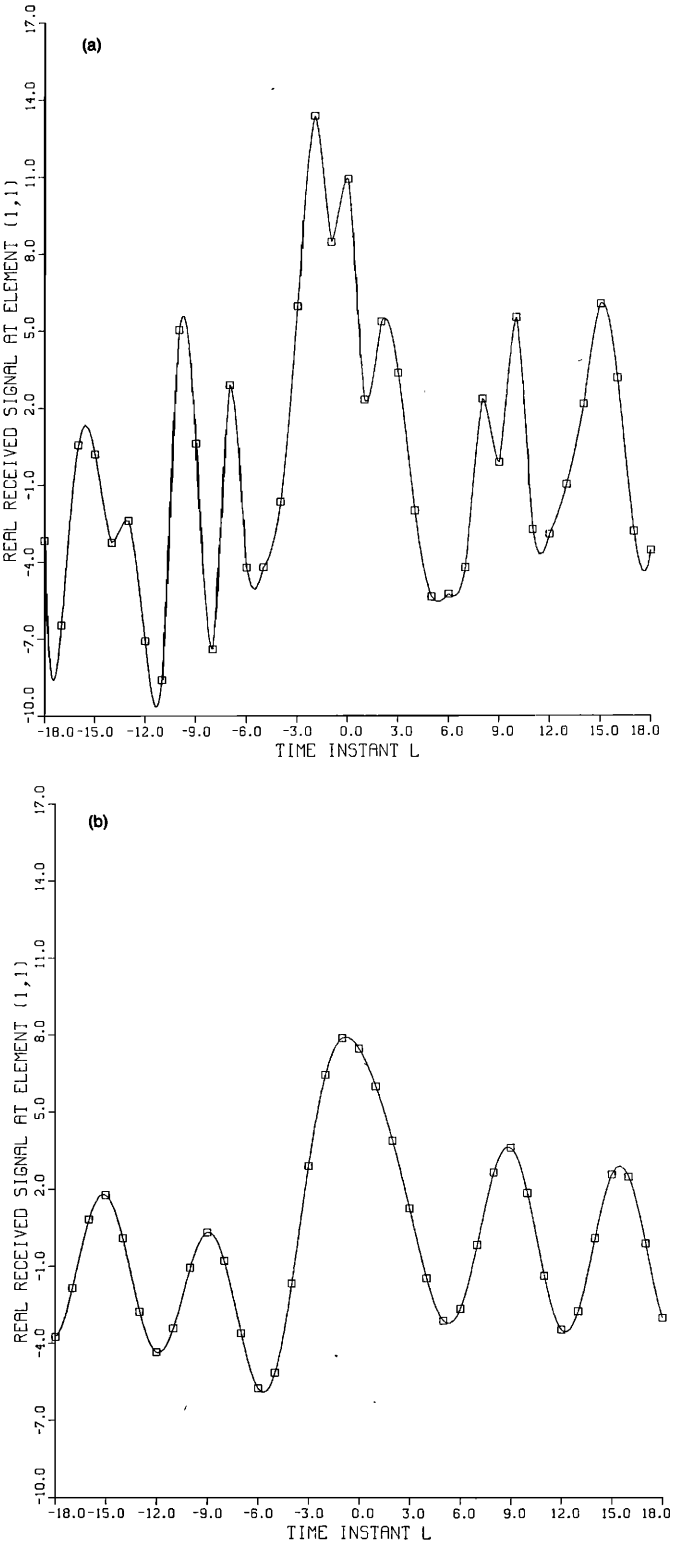

FIG. 3. Real received signal at element (1,1) versus time instant L: (a) case 2: SNR = 0 dB, (b) case 2: no noise.

array of rectangular amplitude weighted point sources used in this article is 100° for $q = 1$ (i.e., 1 kHz) and 14.7° for $q = 6$ (i.e., 6 kHz). The interelement spacings used for case 1 (and case 2) were computed according to Eqs. (40) and (41) with $f_{max} = 6$ kHz and $c = 1500$ m/s. In addition, as the input SNR value was *increased*, *all* estimation errors *decreased* [compare Fig. 2(a) and (b)].

Case 2 corresponds to *three* broadband targets being present. Each general plane-wave field radiated by the three targets was composed of two *unique* harmonics. Target 1 is located at ($\theta_0 = 49°$, $\psi_0 = 38°$) and radiates harmonics $q = 1$ and 6. Target 2 is located at ($\theta_0 = 5°$, $\psi_0 = 137°$) and radiates harmonics $q = 2$ and 5. Target 3 is located at ($\theta_0 = 77°$, $\psi_0 = 307°$) and radiates harmonics $q = 3$ and 4. Since, in this case, there are three incident general plane-wave fields, each with two unique harmonics, the output electrical signal at each element in the array is composed of $K = 6$ harmonics. Therefore, with $K = 6$ and $S = 2, 4$, and 6; *only* $L = 13, 25$, and 37 time samples, respectively, were taken per element. Figure 3(a) and (b) shows a typical output electrical signal at element ($m = 1, n = 1$) in the planar array for an input SNR = 0 dB and for no noise, respectively, corresponding to case 2. Figure 4(a)–(d) illustrates that for a given input SNR value and harmonic number q, the aver-

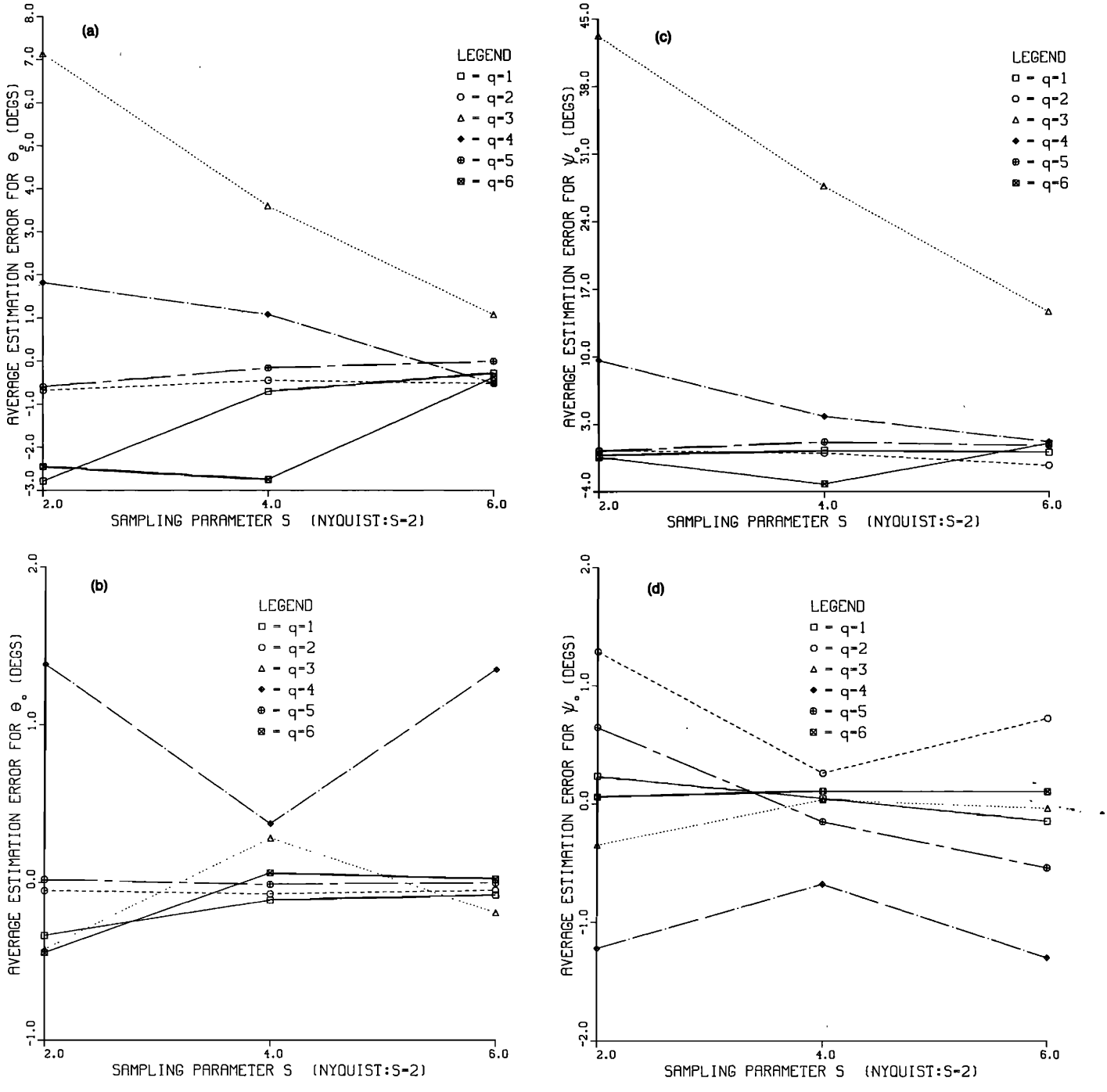

FIG. 4. Average estimation error versus sampling parameter S: (a) case 2: SNR = 0 dB, $I = 100$; (b) case 2: SNR = 9 dB, $I = 100$; (c) case 2: SNR = 0 dB, $I = 100$; (d) case 2: SNR = 9 dB, $I = 100$.

age depression and bearing angle estimation errors *decreased*, in general, as the sampling parameter S *increased*. Similarly, for a given value of S, estimation errors *decreased*, in general, as the harmonic number q associated with a particular target *increased*. As the input SNR value was *increased*, estimation errors, in general, *decreased* [compare Fig. 4(a) and (b) and, Fig. 4(c) and (d)].

Case 3 corresponds to only *one* broadband target being present, located at *end-fire* relative to the planar array, that is, in this case, located at ($\theta_0 = 90°$, $\psi_0 = 90°$). The general plane-wave field radiated by the target was composed of $K = 5$ harmonics. Therefore, with $K = 5$ and $S = 2$, 4, and 6; *only* $L = 11$, 21, and 31 time samples, respectively, were taken per element. Figure 5(a)–(d) illustrates the average depression and bearing angle estimation errors. The results for $q = 5$ were not shown since the estimation errors were on the order of 70°–90°. This poor performance for the highest harmonic at end-fire was explained at the end of Sec. I. The 3-dB beamwidth of the farfield beam pattern of the 7×7 planar array of rectangular amplitude weighted point sources steered to end-fire is 137.6° for $q = 1$ (i.e., 1 kHz) and 58.5° for $q = 5$ (i.e., 5 kHz). The interelement spacings

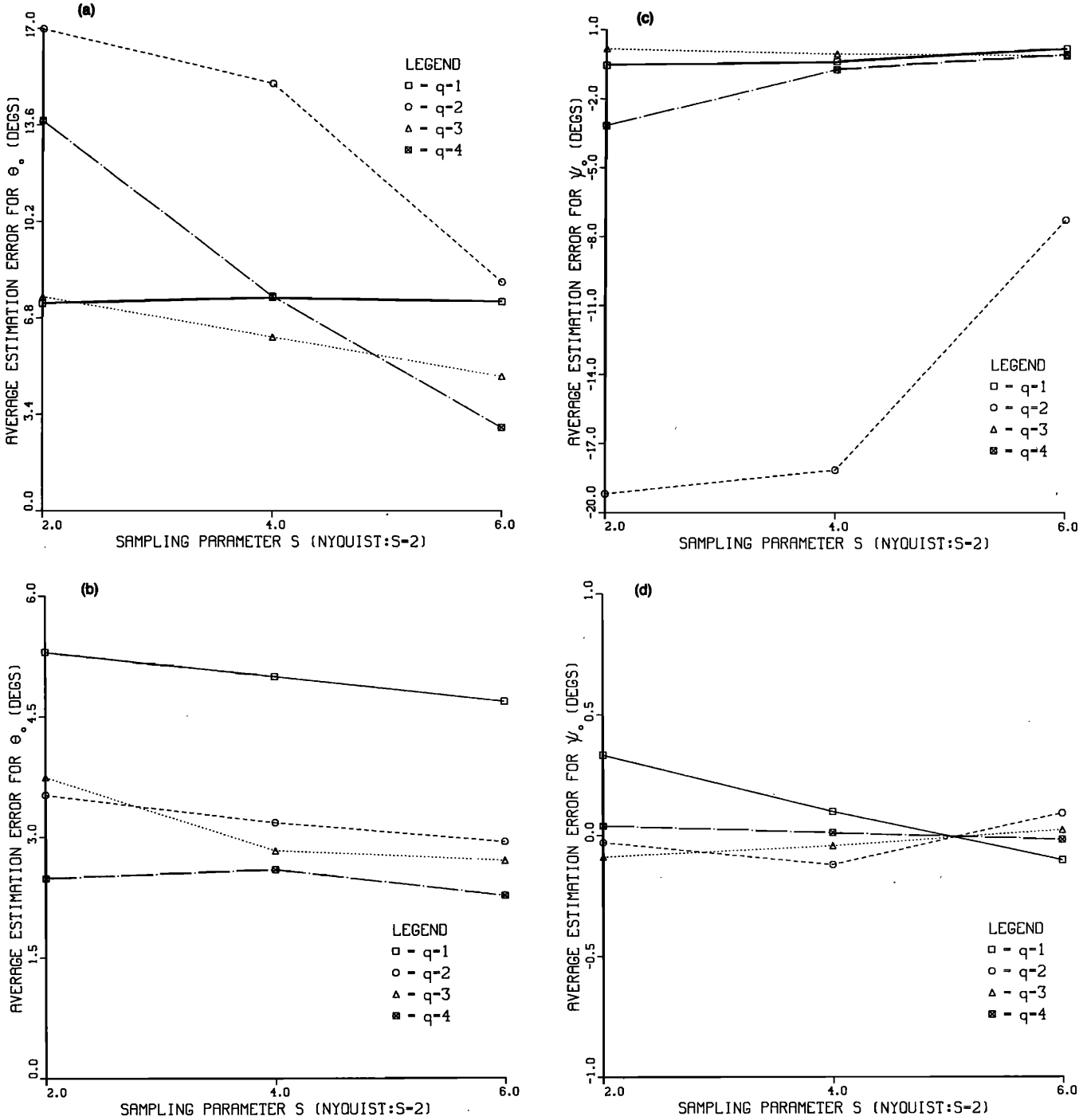

FIG. 5. Average estimation error versus sampling parameter S: (a) case 3: SNR = 0 dB, $I = 100$; (b) case 3: SNR = 9 dB, $I = 100$; (c) case 3: SNR = 0 dB, $I = 100$; (d) case 3: SNR = 9 dB, $I = 100$.

used for case 3 (and case 4) were computed according to Eqs. (40) and (41) with $f_{max} = 5$ kHz and $c = 1500$ m/s.

Case 4 corresponds to *three* broadband targets being present. Each general plane-wave field radiated by the three targets was composed of two harmonics but, this time, two of the three targets shared a common spectral line, namely, the fundamental frequency $f_0 = 1$ kHz. Target 1 is located at ($\theta_0 = 45°$, $\psi_0 = 0°$) and radiates harmonics $q = 1$ and 2. Target 2 is located at ($\theta_0 = 45°$, $\psi_0 = 180°$) and radiates harmonics $q = 1$ and 5. Target 3 is located at ($\theta_0 = 33°$, $\psi_0 = 47°$) and radiates harmonics $q = 3$ and 4. In case 4, $K = 5$ harmonics were used and, as a result, with $S = 2$, 4, and 6; *only* $L = 11$, 21, and 31 time samples, respectively, were taken per element. The computer simulation was run only *once* for case 4 since *no noise* was added to the time samples. The modified complex LMS adaptive algorithm was still allowed 100 iterations. The depression and bearing angle estimation errors for harmonics $q = 2$, 3, 4, and 5 were *zero*. For harmonic $q = 1$, which was the spectral line shared by targets 1 and 2, the beamforming algorithm's estimates were ($\hat{\theta}_0 = 0°$, $\hat{\psi}_0 = 90°$) which places one *false target* exactly in between the two real targets, namely, targets 1 and 2. Therefore, although *all* the real targets were located, one false target was introduced.

[1]L. J. Ziomek and F. Chan, "Frequency Domain Adaptive Beamforming for Planar Arrays," in *Conference Record Twentieth Asilomar Conference on Signals, Systems, and Computers*, 10–12 November 1986, Pacific Grove, CA (IEEE Computer Society, Washington, DC, 1987), pp. 120–124.

[2]L. J. Ziomek and C. D. Behrle, "Localization of Multiple Broadband Targets Via Frequency Domain Adaptive Beamforming for Planar Arrays," in *Conference Record Twenty-First Asilomar Conference on Signals, Systems, and Computers*, 2–4 November 1987, Pacific Grove, CA (Maple, San Jose, CA, 1988).

[3]B. Widrow, J. McCool, and M. Ball, "The Complex LMS Algorithm," Proc. IEEE **63**, 719–720 (1975).

[4]F. A. Reed, P. L. Feintuch, and N. J. Bershad, "Time Delay Estimation using the LMS Adaptive Filter-Static Behavior," IEEE Trans. Acoust. Speech Signal Process. **ASSP-29**, 561–570 (1981).

[5]F. A. Reed, P. L. Feintuch, and N. J. Bershad, "Time Delay Estimation using the LMS Adaptive Filter-Dynamic Behavior," IEEE Trans. Acoust. Speech Signal Process. **ASSP-29**, 571–576 (1981).

[6]F. A. Reed, P. L. Feintuch, and N. J. Bershad, "The Application of the Frequency Domain LMS Adaptive Filter to Split Array Bearing Estimation with a Sinusoidal Signal," IEEE Trans. Acoust. Speech Signal Process. **ASSP-33**, 61–69 (1985).

[7]L. J. Ziomek, *Underwater Acoustics—A Linear Systems Theory Approach* (Academic, Orlando, FL, 1985), pp. 162–166.

[8]See Ref. 7, p. 160.

[9]S. Haykin, "Radar Array Processing for Angle of Arrival Estimation," in *Array Signal Processing*, edited by S. Haykin (Prentice-Hall, Englewood Cliffs, NJ, 1985), pp. 207 and 242.

[10]See Ref. 9, pp. 195–200, 205–207.

[11]S. J. Orfanidis, *Optimum Signal Processing* (MacMillan, New York, 1985), pp. 212–218.

[12]H. Stark and F. B. Tuteur, *Modern Electrical Communications* (Prentice-Hall, Englewood Cliffs, NJ, 1979), pp. 481–483.

[13]See Ref. 7, p. 175.

Localization of multiple broadband targets via frequency domain adaptive beamforming for planar arrays

Lawrence J. Ziomek, and Charles D. Behrle

Citation: The Journal of the Acoustical Society of America **85**, 1236 (1989); doi: 10.1121/1.397454
View online: https://doi.org/10.1121/1.397454
View Table of Contents: http://asa.scitation.org/toc/jas/85/3
Published by the Acoustical Society of America

Articles you may be interested in

Digital Beamforming in the Frequency Domain
The Journal of the Acoustical Society of America **46**, 1089 (1969); 10.1121/1.1911828

A frequency-domain beamforming algorithm for wideband, coherent signal processing
The Journal of the Acoustical Society of America **76**, 1132 (1984); 10.1121/1.391405

Efficient digital beamforming in the frequency domain
The Journal of the Acoustical Society of America **86**, 1813 (1989); 10.1121/1.398614

Application of the fast Fourier transform to broadband beamforming
The Journal of the Acoustical Society of America **98**, 230 (1995); 10.1121/1.413765

Beamforming with microphone arrays for directional sources
The Journal of the Acoustical Society of America **125**, 2098 (2009); 10.1121/1.3089221

Steerable frequency-invariant beamforming for arbitrary arrays
The Journal of the Acoustical Society of America **119**, 3839 (2006); 10.1121/1.2197606